

1 **Title:** An Autonomous Flow Through Salinity and Temperature Perturbation Mesocosm System
2 for Multi-stressor Experiments

3
4 **Author list:** Miller, C.A.^{1,2*}, Urrutti, P.¹, Gattuso, J.-P.^{1,3}, Comeau, S.¹, Lebrun, A.¹, Alliouane¹
5 S., Schlegel, R.W.¹, and F. Gazeau¹

6
7 ¹Sorbonne Université, CNRS, Laboratoire d'Océanographie de Villefranche, 181 chemin du
8 Lazaret, F-06230 Villefranche-sur-Mer, France

9
10 ²Present address: Department of Earth Sciences, Geosciences, Utrecht University, Utrecht, The
11 Netherlands

12
13 ³Institute for Sustainable Development and International Relations, Sciences Po, 27 rue Saint
14 Guillaume, F-75007 Paris, France

15
16
17 **Correspondence to:* Cale A. Miller (e-mail: c.a.miller@uu.nl)

34 **Abstract**

35 The rapid environmental changes in aquatic systems as a result of anthropogenic forcings are
36 creating a multitude of challenging conditions for organisms and communities. The need to
37 better understand the interaction of environmental stressors now, and in the future, is
38 fundamental to determining the response of ecosystems to these perturbations. This work
39 describes an automated *ex-situ* mesocosm perturbation system that can manipulate several
40 variables of aquatic media in a controlled setting. This perturbation system was deployed in
41 Kongsfjorden (Svalbard) where ambient water from the fjord was heated and mixed with
42 freshwater in a multifactorial design to investigate the response of mixed kelp communities in
43 mesocosms to projected future Arctic conditions. The system employed an automated dynamic
44 offset scenario where a nominal temperature increase was programmed as a set value above real-
45 time ambient conditions in order to simulate future warming. A freshening component was
46 applied in a similar manner where a decrease in salinity was coupled to track the temperature
47 offset based on a temperature-salinity relationship in the fjord. The system functioned as an
48 automated mixing manifold that adjusted flow rates of warmed and chilled ambient seawater,
49 with unmanipulated ambient seawater and freshwater delivered as a single source of mixed
50 media to individual mesocosms. These conditions were maintained via continuously measured
51 temperature and salinity in all 12 mesocosms (1 control and 3 treatments, all in triplicates) for 54
52 days. System regulation was robust as median deviations from nominal conditions were < 0.15
53 for both temperature ($^{\circ}\text{C}$) and salinity across the 3 replicates per treatment. Regulation further
54 improved during a second deployment that mimicked three marine heatwave scenarios where a
55 dynamic temperature regulation held median deviations to $< 0.036^{\circ}\text{C}$ from the nominal value for
56 all treatment conditions and replicates. This perturbation system has the potential to be

57 implemented across a wide range of conditions to test single or multi-stressor drivers (e.g.,
58 increased temperature, freshening, high CO₂) while maintaining natural variability. The
59 automated and independent control for each experimental unit (if desired) provides a large
60 breadth of versatility with respect to experimental design.

61

62 **1 Introduction**

63 The persistent burning of fossil fuels since the industrial revolution has radically increased
64 atmospheric CO₂. This has led to an enhanced greenhouse effect resulting in a multitude of
65 changing climatic elements such as increasing sea surface temperature (Bindoff et al., 2019). In
66 fjord systems, the confluence of increased fluvial inputs, glacier and permafrost meltwater,
67 stratification and water mass intrusion, as well as increased sea surface temperatures can create
68 periods of extreme physicochemical conditions for nearshore benthic and pelagic marine
69 communities (Bhatia et al., 2013; Poloczanska et al., 2016; Divya and Krishnan, 2017; Bindoff et
70 al., 2019). As ocean changes progress, the need to better understand the effects of combined
71 stressors (e.g., increased temperature and freshening) on marine communities is essential to
72 understand how community function and species richness will be affected while ecosystems
73 adjust to these new environmental conditions (Kroeker et al., 2017; Wake, 2019; Orr et al.,
74 2020). Several methodological approaches have been used to assess and characterize the
75 response of organisms and communities to future ocean changes, such as *ex-situ*
76 experimentation, the use of natural analogues (e.g., CO₂ vents), and space-for-time substitution
77 (using spatial phenomena to model temporal changes) (Blois et al., 2013; Rastrick et al., 2018;
78 Bass et al., 2021). These approaches, however, can be limited from testing the full range and
79 dynamics of present and future environmental conditions. The use of *ex-situ* experimental

80 systems that manipulate multiple environmental conditions, such as temperature and salinity, can
81 therefore provide a valuable tool to assess the response to multi-stressors in a future ocean.

82 The necessity of conducting multi-stressor experiments has become more pressing due to
83 the increasing interactions of environmental drivers within dynamic systems under a changing
84 climate (Kroeker et al., 2020). Nearshore regions can experience amplified modulations of
85 temperature and salinity on short timescales (Evans et al., 2015; Hales et al., 2016; Fairchild and
86 Hales, 2021). Such instances have been observed in sub-Arctic estuaries where water
87 temperature at a depth of 10 m decreased by 1.5°C in < 10 h, and in temperate systems where the
88 magnitude of salinity change driven by high precipitation displayed a decrease of 4 units in < 24
89 h (Miller and Kelley, 2021; Poppeschi et al., 2021). Changes of this magnitude are particularly
90 pertinent for Arctic fjords, where the variations in salinity from glacial meltwater can influence
91 whether a system exhibits net heterotrophic or autotrophic characteristics (Sejr et al., 2022).

92 Recent advances in the ability to modulate several environmental parameters at once
93 using *ex-situ* mesocosms have been made via the use of modular programmable systems (Wahl
94 et al., 2015; Pansch and Hiebenthal, 2019). Such systems have demonstrated an ability to apply
95 programmable environmental scenarios as a multifactorial design, or as a delta-change (offset)
96 from ambient conditions that mimic the natural variability of an environment. The advantages of
97 these types of automated systems lie in their ability to overcome the need for capturing and
98 measuring abundant discrete measurements used to regulate experimental conditions, and
99 transcend the logistical difficulties of implementing natural variability to experimental designs.
100 In addition, these systems can reduce the need for constant human observation which may be
101 required to program new regulatory operations or make rapid adjustments to experimentally
102 manipulated conditions.

103 Here, we describe an autonomous salinity and temperature experimental perturbation
104 mesocosm system (SalTExPreS) that has the ability to modify, and then regulate, salinity and
105 temperature in real-time. The SalTExPreS can perform similar functions as the *ex-situ* mesocosm
106 systems discussed above (i.e., Kiel-outdoor and -indoor benthocosms), such as applying
107 programmable static or dynamic changes to temperature and salinity, or by replicating natural
108 variability as an offset in real-time, but has the added capability of autonomous control for each
109 experimental unit (e.g., chamber or mesocosm). In the initial deployment of the SalTExPreS, we
110 applied a delta offset (i.e., offset from a measured control) to temperature and salinity as a
111 fractional-factorial treatment design for a two-month long experiment in KongsFjorden,
112 Svalbard, that exposed mixed kelp communities to future temperature, salinity, and irradiance.
113 This study demonstrates the stability and flexibility of the SalTExPreS as an experimental tool to
114 be utilized under extreme and dynamic conditions to test the effects of physicochemical multi-
115 stressors on marine organisms and communities in the context of a multi-month experiment.

116

117 **2 Methods**

118 **2.1 Operational Concept of the Experimental System:**

119

120 The SalTExPreS simulates the drivers in a marine or freshwater system such as temperature,
121 freshening, acidification, or hypoxia as either static or as temporally-variable modifications to a
122 reference water source. This is accomplished by mixing manipulated source water, whether it is
123 freshwater or warmed water, with ambient water through automatic flow valves that control the
124 volume and rate of water delivered. This is regulated by the constant monitoring of the mixed
125 water conditions in each mesocosm or chamber via a programmable feedback loop that transmits
126 the opening or closing of the automatic flow valves. The automated ability of the SalTExPreS is

127 configured to respond to near instantaneous measurements (several reads per second) to achieve
128 high frequency regulation of the manipulated drivers based on a measured *in-situ* or control
129 reference. The programmable nominal conditions in each mesocosm are easily controllable
130 through an intuitive user interface.

131

132 **2.2 Site Description and Experimental Design**

133 Kongsfjorden is a fjord system on the west coast of Svalbard (Norway) where the West
134 Spitsbergen Current exchanges warm Atlantic water through sill channels based on differences in
135 density gradients at the fjord mouth. Over the past two decades, a persistent influx of Atlantic
136 water has resulted in the reduction of sea ice and the melting of marine-terminating glaciers
137 causing enhanced freshwater and fluvial input (Luckman et al., 2015; Tverberg et al., 2019). The
138 influx of freshwater is highest in summer and is accompanied by an important sediment loading
139 with the potential to reduce the euphotic zone from 30 to 0.3 m depth (Svendsen et al., 2002).
140 These climatic changes in the Kongsfjorden environment set a relevant context for the inaugural
141 experiment of the SalTEExPreS. It was placed on a concrete platform situated ~ 12 m from the
142 shoreline in Ny-Ålesund, which is located on southwestern shore of Kongsfjorden ~ 11 km from
143 the fjord mouth.

144 The SalTEExPreS was utilized to implement three treatment scenarios in a fractional-
145 factorial design to simulate expected future conditions in Kongsfjorden for a 54-d experiment
146 that supervised the productivity, survival, and growth response of mixed kelp communities
147 surveyed at 7 m (maximum depth of collection). The treatments were realized by multi-driver
148 combinations of temperature, freshening, and irradiance, where treatments 1 and 2 differed in the
149 magnitude of temperature increase, salinity decrease, and irradiance decrease (Table 1). Only

150 temperature was manipulated for treatment 3. The chosen treatment and salinity perturbations
151 were applied as offset values from *in-situ* fjord conditions, which were measured at an
152 underwater observatory fixed at 11 m depth and captured the natural variability of the fjord
153 system. The applied temperature offsets used for this experiment reflected the projected SSP2-
154 4.5 and SSP5-8.5 scenarios (Meredith et al., 2019; Overland et al., 2019; Table 1). The chosen
155 decreases in salinity were based on correlations between *in-situ* temperature and salinity during
156 summer 2020 in Kongsfjorden (Gattuso et al., 2023), weeks 22 to 35 (Appendix A1 and Fig.
157 A1). These calculated delta salinity values were applied as offsets in treatments 1 and 2 (Table
158 1). The third treatment scenario applied a temperature change of + 5.3°C as a way to decouple
159 the multi-stressor system and evaluate a temperature only stress. The effect of turbidity for
160 treatments 1 and 2 were simulated as a decrease in surface irradiance (i.e., ~ 25% and ~ 40%
161 reduction from ambient irradiance at 7 m) by applying a combination of neutral light and spectral
162 filters (Lee© Filters) placed as static fixtures over the top of the mesocosms. The response of
163 these kelp community assemblages was determined in part by conducting weekly closed system
164 incubations and assessing the growth and metabolism of the kelp in each mesocosm—details and
165 results of this experiment are discussed elsewhere (Lebrun et al. *in review*; Miller et al., *in*
166 *review*).

167

168 **2.3 Experimental System**

169

170 Water was pumped from Kongsfjorden at a 10 m depth (300 m offshore) using a submersible
171 pump (NPS© Albatros F13T) that was tapped into an underwater intake pipe and that fed a
172 header tank in the Kings Bay Marine Laboratory in Ny-Ålesund, Svalbard. To prevent clogging
173 from sediment, the pump was situated at a 10 m depth ensuring a safe height above sediment

174 resuspension from the floor. Pumped ambient seawater from the header tank was then split into
175 three sub-header tanks within the marine lab where ambient water was (1) left unchanged, (2)
176 chilled to 0°C, or (3) warmed to 15°C. Each sub-header tank was plumbed to supply a maximum
177 flow of 6 m³ h⁻¹ for the ambient, 1 m³ h⁻¹ for chilled, and 2 m³ h⁻¹ of warmed water which
178 required a pressure of 0.3 bars for each line to ensure consistent flow rates (Fig. 1). The three
179 control mesocosms received a mix of chilled and ambient seawater in order to properly simulate
180 *in-situ* temperatures. The three experimental treatments (nine mesocosms in total) received a mix
181 of ambient, warmed, and freshwater for treatments 1 and 2, whereas treatment 3 received a mix
182 of just ambient and warmed water (Fig 1). Freshwater was sourced from the tap which is fed by
183 the Tvillingvann reservoir close to Ny-Ålesund. The total flow-through rate of each mesocosm
184 was 0.5 m³ h⁻¹ (i.e., each mesocosm turned over every 2 h) of post-mixed media delivered in an
185 open cycle flow-through system, which was the necessary flow rate needed to maintain the target
186 nominal values. Continuous flow was maintained throughout the experiment except for weekly 3
187 h interruptions (to perform experiments on the community) where the flow to each mesocosm
188 was shut off. In total, there were twelve circular mesocosms (3 treatments and 1 control, each
189 with 3 replicates) with a mean diameter of 1.1 m and a volume of 1 m³, each equipped with a 12
190 W wave pump (Sunsun© JVP-132), a temperature-conductivity probe (Aqualabo, PC4E), an
191 optical oxygen sensor (Aqualabo, PODOC), and an Odyssey© light logger. Fiberglass insulation
192 at the outside of each mesocosm reduced unintended changes in treatment water temperature.

193 Delivery of ambient, chilled, warmed and freshwater first ran through an automated
194 mixing manifold that regulated the flow of each media type assuring that proper volumetric
195 proportions passed through the regulator valves to achieve target conditions (Fig. 1). Each
196 source-water flow line was regulated by an automated 2-way mixing valve (including the

197 incoming freshwater line) which then passed through a 3-way mixing valve that was assigned to
198 each mesocosm (12 in total, Fig. 1). This style of regulation ensured that the proper proportions
199 of manipulated media and ambient water were mixed to achieve nominal conditions. Any
200 temperature variation induced by mixing freshwater was immediately compensated for by
201 regulating the flow of the warm water line. Details regarding the programmed regulation are
202 discussed further in the appendix (Section A2). The mixed media then passed through a flow
203 meter which measured the flow rate to each mesocosm. A hand-crank regulating valve was
204 placed directly after the flow meter and was used for making minor adjustments and controlling
205 the overall flow. Measurements by the pressure sensors, the status of open position for the
206 regulator valves, and flow rates were logged every minute and displayed on the user interface
207 (Fig. A3).

208

209 **2.4 Nominal Regulation**

210

211 Nominal temperature conditions of + 3.3, 5.3, and 5.3°C applied to treatments 1, 2, and 3,
212 respectively, were offsets from the nominal control temperature. The nominal temperature of the
213 control was updated hourly and programmed to replicate the measured *in-situ* conditions in the
214 fjord logged by the AWIPEV (Alfred Wegener Institute and Institute Paul Emile Victor)
215 FerryBox part of the COSYNA underwater observatory (<https://dashboard.awi.de/>) situated at a
216 depth of 11 m. Each treatment condition (temperature and salinity offset) was set by manually
217 programming the nominal value of temperature in the software interface (see appendix A3). The
218 salinity offset was coupled to the nominal temperature via the correlation described in appendix
219 A1. The measured temperature and salinity observations from inside each mesocosm were
220 recorded multiple times per minute and used to continuously monitor the regulation of the

221 conditions inside each mesocosm. This data transmission was used to program the software
222 controller that performed the automated regulation of mixed media (for details see appendix A2).

223 224 **2.5 Software**

225 The software application used for the control of the SalTExPreS was developed using Visual
226 Studio Community (2019 edition) with the vMicro extension and Arduino 1.8.13. The program
227 application has a user-friendly interface designed to allow real-time monitoring and
228 parameterization of regulation processes (Fig. A3). The main window displays each mesocosm
229 condition (the parameters measured by a sensor), their piping connections, a connection status
230 for each Programmable Logic Controller (PLC) informing on proper communication, date and
231 time of the last received communication packet from the Head PLC, and the status of the
232 experiment (e.g., started or stopped). The interface also displays the valve opening percentage
233 along with the nominal pressure and the actual measured value for each main source-water inlet.
234 In addition, the *in-situ* data (temperature and salinity) received from the FerryBox is displayed
235 with the time and date of the last logged value utilized to program the real-time nominal value of
236 the control. Sensor readings of flow rate (L min^{-1}), O_2 saturation (%), salinity, and temperature
237 ($^{\circ}\text{C}$) are shown for each mesocosm in conjunction with the treatment nominal values (i.e.,
238 temperature, and salinity when relevant). All measured data are stored through the server
239 connection to the cloud, however, there is a backup microSD card on the Head PLC that logs
240 data from all mesocosms every 5 sec. If communication fails between the Head PLC and the
241 interfaced computer, data will not be retrieved by the PC during the communication break but
242 will be retained by the microSD card.

243 244 **3 Results**

245
246
247
248
249
250
251
252
253
254
255
256
257
258
259
260
261
262
263
264
265
266
267
268
269
270
271

3.1 Regulation of the Control

The control was able to simulate the ambient fjord temperature well over the experimental period where the average value across the 3 replicates deviated $< 0.3^{\circ}\text{C}$ (Table 2, Fig. 2). The overall quality of the regulation was achieved by the ability of the system to interpret and respond to the measured data from the FerryBox (or to follow a manually programmed nominal value when communication with the FerryBox was interrupted). During the experiment, the FerryBox went intermittently offline 24% of the time, ceasing transmission of real-time data that resulted in a break of communication to the PLCs. This somewhat frequent break in communication resulted in an average nominal deviation that was nearly double for the control compared to the treatment conditions (Table 2). The ability to manually program a new nominal value when communication breaks occurred ensured that the control remained robustly regulated. Over the entire period of the SalTEPreS deployment, the mean temperature of the control increased from ~ 4 to 6.5°C from early July to the end of August (Fig. 3a). The coldest mean temperature of the control occurred when a backup pump situated at 90 m depth in the fjord was used from 2021-07-14 $\sim 21:00$ UTC until 2021-07-26 13:49 UTC while the original pump at 10 m depth was repaired. During this period, the control was $\sim 1.0 - 1.5^{\circ}\text{C}$ cooler than the temperature measured by the FerryBox (Figs. 2, 3). Since a warmed seawater inlet was not supplied to the control, the temperature of the control remained cooler than the measured ambient conditions at the FerryBox. Despite the cooler temperature for the control, regulation of flow rates, mesocosm turnover time, and variability across the control replicates was well maintained by the system.

1.2 Temperature and Salinity Regulation

272
273 The regulation of temperature and salinity in the different treatment conditions (Trts. 1 – 3) was
274 maintained by the SalTExPreS for the full planned duration of 54 days (2021-07-03 to 2021-08-
275 26). For the first 6 days of the SalTExPreS experiment, the treatment conditions were held at the
276 control (i.e., no applied offset from the control) before the stepwise increase in temperature
277 began. On 2021-07-10 12:00 UTC a temperature offset of $0.55^{\circ}\text{C d}^{-1}$ was programmed for
278 treatment 1 while treatment 2 and 3 were programmed to increase by $0.88^{\circ}\text{C d}^{-1}$ (Figs. 2, 3). The
279 final nominal temperature above the control was reached on 2021-07-15 21:00 UTC. The system
280 needed 4 h to achieve the new temperature conditions (i.e., homogenize the mesocosm to a
281 0.88°C increase). A manual override was applied to the salinity regulation for treatments 1 and 2
282 which resulted in the system achieving the final salinity offset value upon the initial temperature
283 increase (Fig. 3b, 4). This was done to ensure the maintenance of salinity regulation as the
284 temperature offsets were applied relative to the control, which was receiving fjord water pumped
285 from 90 m and was colder than the measured *in-situ* conditions. It took the system 4 h to achieve
286 the salinity offset for treatment 2 adjusting the value from ~ 34 to 29.8 (Fig. 3b, 4).

287 The precision of the temperature and salinity regulation across all treatment conditions
288 was well maintained as the mean difference between the measured value and the nominal value
289 was $< 0.2^{\circ}\text{C}$ and < 0.36 for salinity across the entire deployment (Table 2). The mean deviations
290 observed across treatments did not appear to correlate to the degree of offset. Thus, treatment 3
291 showed the highest precision for temperature regulation, while salinity regulation was the most
292 robust for treatment 2 compared to treatment 1 (Table 2). During several instances when
293 communication was interrupted between the FerryBox and the Head PLC, the SalTExPreS
294 retained the last measured value at the FerryBox as a contingency protocol. This aided in the
295 ability of the system to maintain a high degree of regulation throughout the entire deployment.

296 The largest deviation from the nominal value for all treatment conditions occurred during the
297 single instance in which the last read value from the FerryBox was not retained: this occurred on
298 2021-08-24 04:47 UTC (Fig. 4). Communication was quickly restored after this incident by
299 cycling the program code, and the average deviation of temperature ($^{\circ}\text{C}$) and salinity for
300 treatment 1 for the remainder of the deployment was < 0.16 , and < 0.25 for treatment 2.

301 When adequate flow rates were maintained, the SalTExPreS was able to simultaneously
302 regulate 12 mesocosms at 4 different conditions to deviations in temperature and salinity that
303 were $< 0.5^{\circ}\text{C}$ or 0.5 in salinity from the nominal value $\geq 80\%$ and $\geq 70\%$ of the time,
304 respectively (Fig. 5). Due to an erroneous nominal value for the control during the 90 m pump
305 usage, these times were excluded. If warm water could have been mixed with the ambient water
306 feeding the control mesocosms, then a proper nominal value could have been maintained. Over
307 the full duration of the experiment, effective regulation from the nominal temperature and
308 salinity values were kept to < 1 for all mesocosms 89% of the time for temperature ($^{\circ}\text{C}$), and
309 80% for the salinity (excluding the 1st replicate for treatment 2).

310

311 **Discussion**

312

313 The first application of the fully autonomous SalTExPreS demonstrated the capacity of the
314 system to successfully manipulate temperature and salinity as an offset value from the control,
315 thus maintaining, natural, *in-situ* variability for 4 different conditions simultaneously. We
316 utilized this deployment to test the effects of climate change drivers on Arctic kelp communities
317 recognizing the feasibility of the system to perform *ex-situ* experiments on organisms or whole
318 communities (Miller et al., *in review*). The versatility of the system not only allows for the
319 manipulation of temperature and salinity, but can incorporate other factors such as CO_2 or

320 hypoxia (Gazeau et al., *in prep*). While this experiment used a control offset approach to produce
321 treatment conditions, programmable parametrization of various treatment combinations can be
322 applied depending on the question and design of the experiment. The automated component of
323 the system reduced the logistical hurdles that can arise when performing high precision
324 replication and regulation of experimental conditions that track real-time system variability.
325 While the use of such a system can reduce user oversight and limitations, there is still a need for
326 diligent operation.

327 Since the initial experiment, we have implemented a number of changes to improve the
328 performance of the system which have been realized during a second experiment in the summer
329 of 2022 (Fig. 6). In this experiment, the SalTExPreS was integrated to function with a deployable
330 heat pump to simulate multiple scenarios of marine heatwave patterns over a nearly month-long
331 experiment. In this instance, temperature regulation was vastly improved as a result of the
332 programmable modifications made since the initial experiment. During this second experiment,
333 the SalTExPreS mimicked 3 marine heatwave scenarios where a dynamic temperature regulation
334 kept deviations in the 9 different mesocosms at $< 0.5^{\circ}\text{C}$ for 94% of the time. This was an
335 improvement to the % time of temperature regulation by $\sim 15\%$ compared to the first
336 experiment. During the first experiment, inconsistent flow rates and communication errors
337 between the FerryBox and the Head PLC were the primary causes of larger deviations (> 2.0
338 salinity or $^{\circ}\text{C}$) from nominal values. For example, flow rates of $< 2 \text{ L min}^{-1}$ accounted for $\sim 20\%$
339 of the large deviations in temperature and salinity regulation. Simple software modifications
340 such as ‘pop-up’ alert windows that warned when a lapse in communication with the FerryBox
341 occurred (e.g., FerryBox stopped logging), and the addition of contingency coding instructions
342 (i.e., fail-safe instructions) ensuring that the last received *in-situ* data were maintained solved

343 most of the issues. Communication errors were easily remedied by cycling the power on a PLC,
344 which is why pop-up alerts were an improvement to the operation. Other extraneous
345 circumstances that could impact flow rates, such as pump failure and clogging of the seawater
346 intake ports, are issues that need to be addressed whenever the SalTExPreS is used. However,
347 these are very manageable situations which can be easily mitigated by an operator.

348 The novelty of the SalTExPreS lies in its ability to independently regulate experimental
349 conditions in a single experimental chamber (e.g., mesocosm). The operational data produced
350 from this deployment are reliable, easily quantifiable, and provide the highest degree of
351 monitoring frequency for every applied experimental condition. This study has demonstrated the
352 system's ability to replicate dynamic nearshore environments where temperature and salinity can
353 vary at high frequency (e.g., tidally). The system's additional capacity to mimic future scenarios
354 by applying an amplitude offset to the natural dynamics of *in-situ* conditions is an added feature
355 for conducting manipulative experiments. Wahl et al. (2015) described a system with a similar
356 capability, but regulated treatment conditions by monitoring source water and adjusting that
357 media before it was delivered to each experimental chamber. The SalTExPreS differs in that it
358 measures the conditions inside each experimental chamber (i.e., mesocosm) and regulates them
359 independently based on per second measurements. This provides the flexibility to individually
360 modulate each experimental chamber providing a broad range of versatility. The lack of
361 infrastructure needed to set up the SalTExPreS makes it easy to deploy and transport. As long as
362 there is a sufficient supply of ambient water and manipulated media, there is little limit to the
363 versatility of automated control for each mesocosm. Many research endeavors and future
364 implementations by the SalTExPreS have the potential to conduct a large range of experimental
365 settings that pertain to environmental perturbations associated with climate change or other

366 anthropogenic forcings. The operation of such a system in extreme environmental conditions has
367 shown the durability of the manifold to endure an adverse Arctic summer and still respond
368 without mechanical failures. With proper operation and user proficiency, this proves to be a
369 highly sophisticated and powerful tool to be utilized for marine and aquatic perturbation
370 experiments.

371

372 **Acknowledgements**

373 This study is part of the FACE-IT Project (The Future of Arctic Coastal Ecosystems –
374 Identifying Transitions in Fjord Systems and Adjacent Coastal Areas). The authors thank Jens
375 Terhaar for helping with temperature projection data, Philipp Fischer for access to the AWIPEV
376 data as well as AWIPEV and Kings Bay staff for helping with logistical details, shipping, and
377 access to the marine lab facilities.

378

379 **Author contributions**

380 C.M. and F.G. conceptualized the frame of the paper while F.G, S.C, and P.U. designed the
381 experimental system. P.U. programmed the software. C.M. wrote the manuscript, performed the
382 data analysis, and constructed the figures and tables while P.U. designed schematic figures. All
383 authors participated in the operation of the system and have, thus, commented, and edited during
384 writing.

385

386 **Financial support**

387 This study was conducted in the frame of the project FACE-IT (The Future of Arctic Coastal
388 Ecosystems – Identifying Transitions in Fjord Systems and Adjacent Coastal Areas). FACE-IT

389 has received funding from the European Union’s Horizon 2020 research and innovation
390 programme under grant agreement No 869154. Logistical and financial support was provided by
391 IPEV, The French Polar Institute and the Foundation Prince Albert 2 of Monaco (project: 3051,
392 <http://fpa2.org>).

393

394 **Competing interest**

395 The authors declare no competing interests exist.

396 **References**

397 Bass, A., Wernberg, T., Thomsen, M., and Smale, D.: Another Decade of Marine Climate
398 Change Experiments: Trends, Progress and Knowledge Gaps, *Frontiers in Marine Science*, 8,
399 2021.

400 Bhatia, M. P., Kujawinski, E. B., Das, S. B., Breier, C. F., Henderson, P. B., and Charette, M. A.:
401 Greenland meltwater as a significant and potentially bioavailable source of iron to the ocean,
402 *Nature Geosci*, 6, 274–278, <https://doi.org/10.1038/ngeo1746>, 2013.

403 Bindoff, N. L., Cheung, W. W. L., Kairo, J. G., Arístegui, J., Guinder, V. A., Hallberg, R.,
404 Hilmi, N., Jiao, N., Karim, M. S., Levin, L., O’Donoghue, S., Purca Cuicapusa, S. R., Rinkevich,
405 B., Suga, T., Tagliabue, A., and Williamson, P.: Chapter 5: Changing Ocean, Marine
406 Ecosystems, and Dependent Communities — Special Report on the Ocean and Cryosphere in a
407 Changing Climate, 2019.

408 Blois, J. L., Williams, J. W., Fitzpatrick, M. C., Jackson, S. T., and Ferrier, S.: Space can
409 substitute for time in predicting climate-change effects on biodiversity, *Proc Natl Acad Sci U S*
410 *A*, 110, 9374–9379, <https://doi.org/10.1073/pnas.1220228110>, 2013.

411 Divya, D. T. and Krishnan, K. p.: Recent variability in the Atlantic water intrusion and water
412 masses in Kongsfjorden, an Arctic fjord, *Polar Science*, 11, 30–41,
413 <https://doi.org/10.1016/j.polar.2016.11.004>, 2017.

414 Evans, W., Mathis, J. T., Ramsay, J., and Hetrick, J.: On the frontline: Tracking ocean
415 acidification in an Alaskan shellfish hatchery, *PLOS ONE*, 10, e0130384,
416 <https://doi.org/10.1371/journal.pone.0130384>, 2015.

417 Fairchild, W. and Hales, B.: High-Resolution Carbonate System Dynamics of Netarts Bay, OR
418 From 2014 to 2019, *Frontiers in Marine Science*, 7, 2021.

419 Gattuso, J.-P., Alliouane, S., and Fischer, P.: High-frequency, year-round time series of the
420 carbonate chemistry in a high-Arctic fjord (Svalbard), *Earth System Science Data*, 15, 2809–
421 2825, <https://doi.org/10.5194/essd-15-2809-2023>, 2023.

422 Hales, B., Suhrbier, A., Waldbusser, G. G., Feely, R. A., and Newton, J. A.: The Carbonate
423 Chemistry of the “Fattening Line,” Willapa Bay, 2011–2014, *Estuaries and Coasts*, 1–14,
424 <https://doi.org/10.1007/s12237-016-0136-7>, 2016.

425 Kroeker, K. J., Kordas, R. L., and Harley, C. D. G.: Embracing interactions in ocean
426 acidification research: confronting multiple stressor scenarios and context dependence, *Biology*
427 *Letters*, 13, 20160802, <https://doi.org/10.1098/rsbl.2016.0802>, 2017.

428 Kroeker, K. J., Bell, L. E., Donham, E. M., Hoshijima, U., Lummis, S., Toy, J. A., and Willis-
429 Norton, E.: Ecological change in dynamic environments: Accounting for temporal environmental
430 variability in studies of ocean change biology, *Global Change Biology*, 26, 54–67,
431 <https://doi.org/10.1111/gcb.14868>, 2020.

432 Lebrun, A., Miller, C. A., Meynadier, M., Comeau, S., Urrutti, P., Alliouane, S., Schlegel, R.,
433 Gattuso, J.-P., and Gazeau, F.: Multifactorial effects of warming, low irradiance, and low salinity
434 on Arctic kelps, *EGUsphere* [preprint], <https://doi.org/10.5194/egusphere-2023-1875>, *in review*.
435

436 Luckman, A., Benn, D. I., Cottier, F., Bevan, S., Nilsen, F., and Inall, M.: Calving rates at
437 tidewater glaciers vary strongly with ocean temperature, *Nat Commun*, 6, 8566,
438 <https://doi.org/10.1038/ncomms9566>, 2015.

439 Meredith, M., Sommerkon, M., Cassotta, S., Derksen, C., Ekaykin, A., Hollowed, A., Kofinas,
440 G., Mackintosh, A., Melbourne-Thomas, J., Muelbert, M. M. C., Ottersen, G., Ptitchard, H., and
441 Schuur, E. A. G.: Chapter 3: Polar regions — Special Report on the Ocean and Cryosphere in a
442 Changing Climate, IPCC, 2019.

443 Miller, C., Gazeau, F., Lebrun, A., Gattuso, J.-P., Alliouane, S., Urrutti, P., Schlegel, R., and
444 Comeau, S.: Productivity of Mixed Kelp Communities in an Arctic Fjord Exhibit Tolerance to a
445 Future Climate, <https://doi.org/10.2139/ssrn.4563719>, *in review*.

446 Miller, C. A. and Kelley, A. L.: Seasonality and biological forcing modify the diel frequency of
447 nearshore pH extremes in a subarctic Alaskan estuary, *Limnology and Oceanography*, 66, 1475–
448 1491, <https://doi.org/10.1002/lno.11698>, 2021.

449 Orr, J. A., Vinebrooke, R. D., Jackson, M. C., Kroeker, K. J., Kordas, R. L., Mantyka-Pringle,
450 C., Van den Brink, P. J., De Laender, F., Stoks, R., Holmstrup, M., Matthaei, C. D., Monk, W.
451 A., Penk, M. R., Leuzinger, S., Schäfer, R. B., and Piggott, J. J.: Towards a unified study of
452 multiple stressors: divisions and common goals across research disciplines, *Proceedings of the*
453 *Royal Society B: Biological Sciences*, 287, 20200421, <https://doi.org/10.1098/rspb.2020.0421>,
454 2020.

455 Overland, J., Dunlea, E., Box, J. E., Corell, R., Forsius, M., Kattsov, V., Olsen, M. S., Pawlak, J.,
456 Reiersen, L.-O., and Wang, M.: The urgency of Arctic change, *Polar Science*, 21, 6–13,
457 <https://doi.org/10.1016/j.polar.2018.11.008>, 2019.

458 Pansch, C. and Hiebenthal, C.: A new mesocosm system to study the effects of environmental
459 variability on marine species and communities, *Limnology and Oceanography: Methods*, 17,
460 145–162, <https://doi.org/10.1002/lom3.10306>, 2019.

461 Poloczanska, E. S., Burrows, M. T., Brown, C. J., García Molinos, J., Halpern, B. S., Hoegh-
462 Guldberg, O., Kappel, C. V., Moore, P. J., Richardson, A. J., Schoeman, D. S., and Sydeman, W.
463 J.: Responses of Marine Organisms to Climate Change across Oceans, *Frontiers in Marine*
464 *Science*, 3, 2016.

465 Poppeschi, C., Charria, G., Goberville, E., Rimmelin-Maury, P., Barrier, N., Petton, S.,
466 Unterberger, M., Grossteffan, E., Repecaud, M., Quémener, L., Theetten, S., Le Roux, J.-F., and
467 Tréguer, P.: Unraveling Salinity Extreme Events in Coastal Environments: A Winter Focus on
468 the Bay of Brest, *Frontiers in Marine Science*, 8, 2021.

469 Rastrick, S. S. P., Graham, H., Azetsu-Scott, K., Calosi, P., Chierici, M., Fransson, A., Hop, H.,
470 Hall-Spencer, J., Milazzo, M., Thor, P., and Kutti, T.: Using natural analogues to investigate the
471 effects of climate change and ocean acidification on Northern ecosystems, *ICES Journal of*
472 *Marine Science*, 75, 2299–2311, <https://doi.org/10.1093/icesjms/fsy128>, 2018.

473 Sejr, M. K., Bruhn, A., Dalsgaard, T., Juul-Pedersen, T., Stedmon, C. A., Blicher, M., Meire, L.,
474 Mankoff, K. D., and Thyrring, J.: Glacial meltwater determines the balance between autotrophic
475 and heterotrophic processes in a Greenland fjord, *Proceedings of the National Academy of*
476 *Sciences*, 119, e2207024119, <https://doi.org/10.1073/pnas.2207024119>, 2022.

477 Svendsen, H., Beszczynska-Møller, A., Hagen, J. O., Lefauconnier, B., Tverberg, V., Gerland,
478 S., Børre Ørbæk, J., Bischof, K., Papucci, C., Zajaczkowski, M., Azzolini, R., Bruland, O., and
479 Wiencke, C.: The physical environment of Kongsfjorden–Krossfjorden, an Arctic fjord system in
480 Svalbard, *Polar Research*, 21, 133–166, <https://doi.org/10.3402/polar.v21i1.6479>, 2002.

481 Tverberg, V., Skogseth, R., Cottier, F., Sundfjord, A., Walczowski, W., Inall, M. E., Falck, E.,
482 Pavlova, O., and Nilsen, F.: The Kongsfjorden Transect: Seasonal and Inter-annual Variability in
483 Hydrography, in: *The Ecosystem of Kongsfjorden, Svalbard*, edited by: Hop, H. and Wiencke,
484 C., Springer International Publishing, Cham, 49–104, [https://doi.org/10.1007/978-3-319-46425-](https://doi.org/10.1007/978-3-319-46425-1_3)
485 [1_3](https://doi.org/10.1007/978-3-319-46425-1_3), 2019.

486 Wahl, M., Buchholz, B., Winde, V., Golomb, D., Guy-Haim, T., Müller, J., Rilov, G., Scotti, M.,
487 and Böttcher, M. E.: A mesocosm concept for the simulation of near-natural shallow underwater
488 climates: The Kiel Outdoor Benthocosms (KOB), *Limnology and Oceanography: Methods*, 13,
489 651–663, <https://doi.org/10.1002/lom3.10055>, 2015.

490 Wake, B.: Experimenting with multistressors, *Nat. Clim. Chang.*, 9, 357–357,
491 <https://doi.org/10.1038/s41558-019-0475-z>, 2019.

492 Ziegler, J. G. and Nichols, N. B.: Optimum Settings for Automatic Controllers, *Transactions of*
493 *the American Society of Mechanical Engineers*, 64, 759–765, <https://doi.org/10.1115/1.4019264>,
494 1943.

495

496 **Tables**

497 **Table 1.** Experimental treatment conditions with corresponding offsets (as compared to the
 498 control) for temperature (°C), salinity and photosynthetically active radiation (PAR; expressed as
 499 a percentage). See section A1 and figure A1 for a full description of the temperature-salinity
 500 relationship used to calculate salinity offsets.

| <i>Treatment</i> | <i>Temperature</i> | <i>Salinity</i> | <i>PAR</i> |
|------------------|--------------------|--------------------------------------|------------|
| 1 | + 3.3 °C | - 2.5 – 3.0 - S = 0.546*T + 0.490 | - 25% PAR |
| 2 | + 5.3 °C | - 5.0 – 5.5 - S = 0.877*T + 0.089 | - 40% PAR |
| 3 | + 5.3 °C | Ambient | Ambient |

501

502

503

504

505

506

507

508

509

510

511

512

513

514

515 **Table 2.** Absolute mean difference between measured temperature (T_{meas} ; °C) and salinity (S_{meas})
516 values against nominal values (T_{nominal} and S_{nominal}) plus or minus the corresponding standard
517 deviation, in each mesocosm during the experimental period. A weighted average was used for
518 treatments 1 – 3 to account for the initial 5-day incremental increase. Triplicate mesocosms per
519 condition are expressed as a, b and c. Water mixture indicates the types of media supplied to
520 each treatment, denoted with an ‘x’.

| <i>Treatment</i> | <i>Mean diff</i> | | <i>Water mixture</i> | | | |
|---------------------|---|---|----------------------|----------------|-------------|--------------|
| | <i>Abs($T_{\text{meas}} - T_{\text{nominal}}$)</i> | <i>Abs($S_{\text{meas}} - S_{\text{nominal}}$)</i> | <i>Cold</i> | <i>Ambient</i> | <i>Warm</i> | <i>Fresh</i> |
| <i>Control a</i> | 0.275 ± 0.39 | – | x | x | | |
| <i>Control b</i> | 0.291 ± 0.36 | – | x | x | | |
| <i>Control c</i> | 0.223 ± 0.36 | – | x | x | | |
| <i>Treatment 1a</i> | 0.126 ± 0.31 | 0.116 ± 0.31 | | x | x | x |
| <i>Treatment 1b</i> | 0.142 ± 0.29 | 0.148 ± 0.22 | | x | x | x |
| <i>Treatment 1c</i> | 0.145 ± 0.33 | 0.171 ± 0.33 | | x | x | x |
| <i>Treatment 2a</i> | 0.111 ± 0.29 | 0.357 ± 0.74 | | x | x | x |
| <i>Treatment 2b</i> | 0.133 ± 0.29 | 0.149 ± 0.26 | | x | x | x |
| <i>Treatment 2c</i> | 0.196 ± 0.38 | 0.128 ± 0.25 | | x | x | x |
| <i>Treatment 3a</i> | 0.109 ± 0.27 | – | | x | x | |
| <i>Treatment 3b</i> | 0.112 ± 0.27 | – | | x | x | |
| <i>Treatment 3c</i> | 0.106 ± 0.28 | – | | x | x | |

521

522

523

524

525

526

527

528

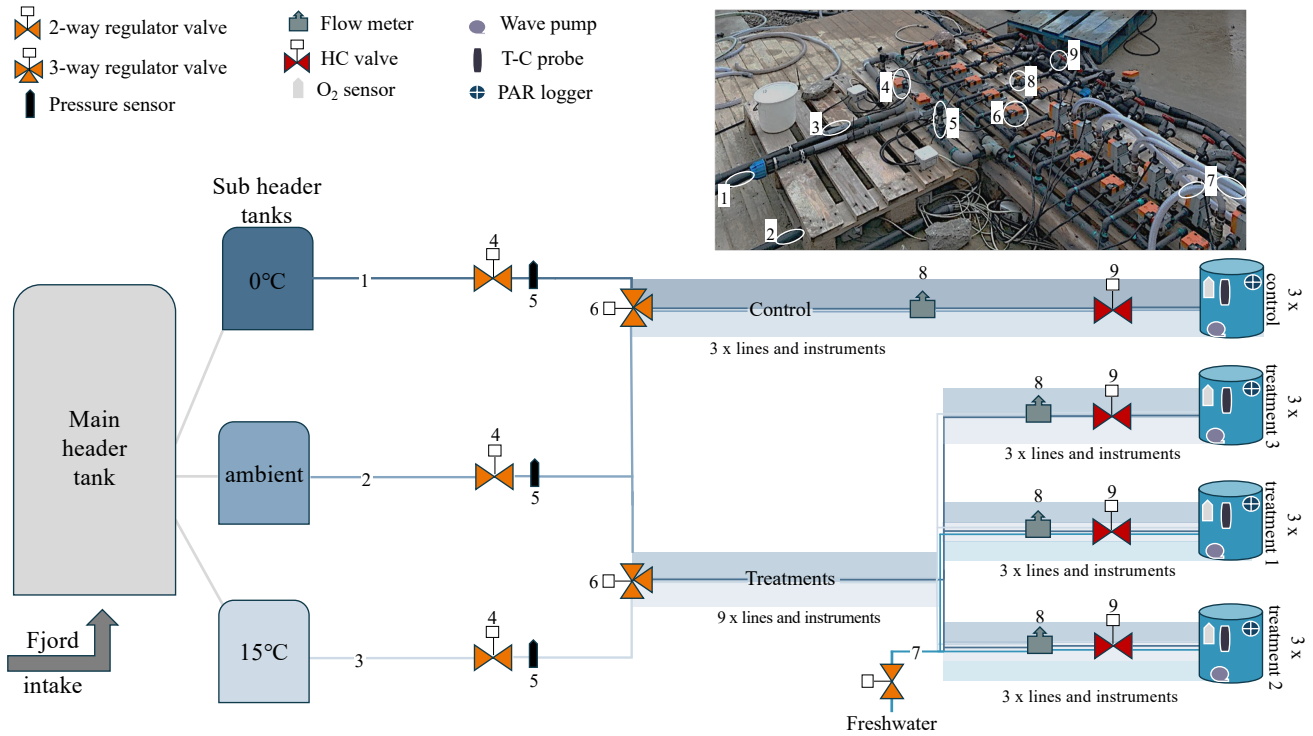
529

530

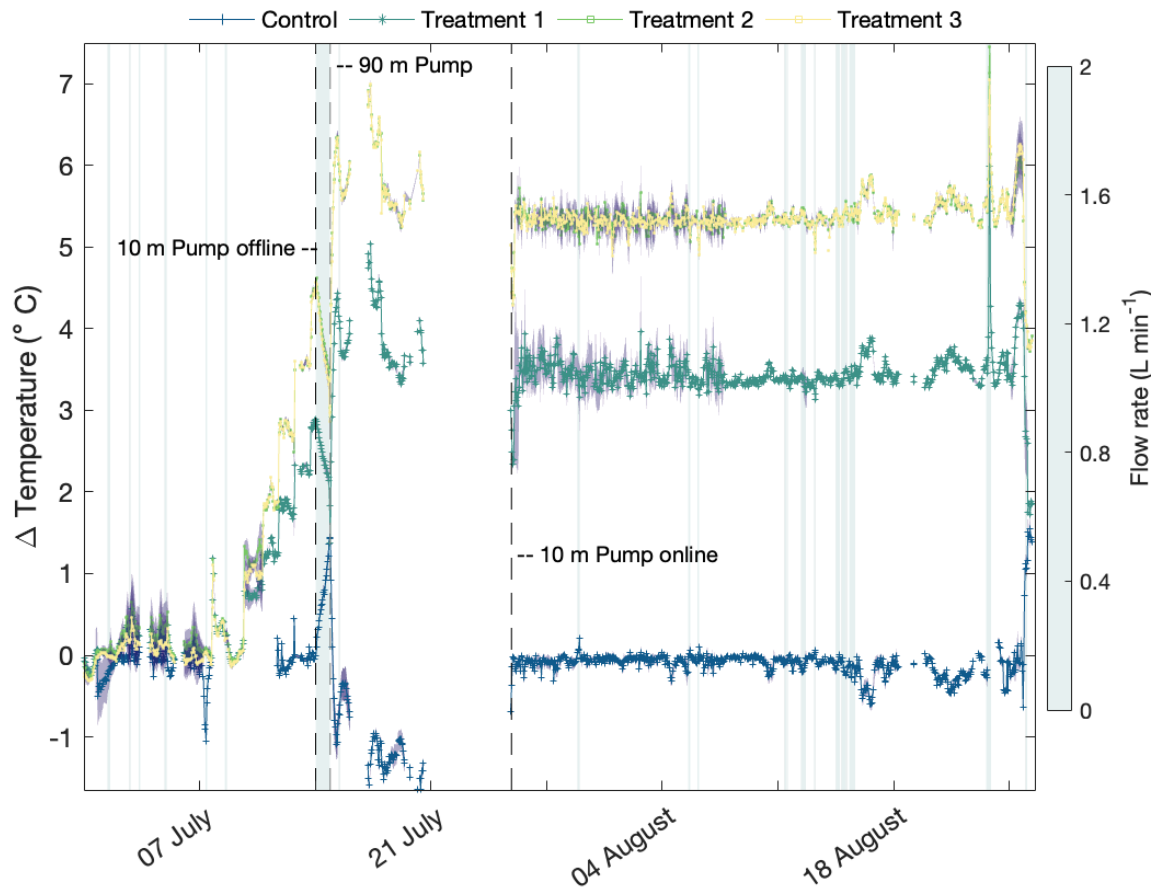
531

532

533 **Figures**



535 **Figure 1.** Piping schematic of the SaITeXPreS which includes the mixing and regulation
 536 manifold. Items 1 – 3 depict the main seawater inlets from the chilled, ambient, and warmed sub-
 537 header tanks located in the Kings Bay Marine Laboratory. Seawater from each sub-header tank
 538 moves through a 2-way regulator (4) valve followed by a pressure sensor (5) before splitting into
 539 individual lines that lead to all 12 3-way regulator valves (6), each assigned to a single
 540 mesocosm. For treatments 1 and 2, the freshwater inlet (clear tube; item 7) passes through a 2-
 541 way regulator valve before mixing with the ambient and warmed seawater lines. Flow rates are
 542 then measured (8) post-mixing, and final flow rates are set using a hand-crank (HC) red valve
 543 (9). The shaded regions in the schematic indicate that mixed media lines and instruments occur
 544 3x or 9x times. T-C probe is the temperature-conductivity probe and the PAR logger measures
 545 the photosynthetically active radiation. Photos of mesocosms and the sensors inside can be found
 546 in the appendix (Fig. A6). Table A1 provides the parts list for the items shown in this figure.



548

549 **Figure 2.** The hourly mean (across triplicated mesocosms) temperature offsets of all applied
 550 conditions. For control mesocosms (in blue), offsets were calculated against *in-situ*
 551 measurements (FerryBox). For the three experimental treatments (dark green, light green, and
 552 yellow for treatments 1, 2 and 3, respectively), offsets were estimated against the mean control
 553 values. The purple shaded region around the mean is the standard deviation. The heatmap
 554 isoclines (blue-grey shaded regions) are instances when flow rates were $\leq 2 \text{ L min}^{-1}$ (threshold to
 555 avoid large deviations > 2.0 salinity or $^{\circ}\text{C}$). Dashed black lines indicate periods when the pump
 556 at 10 m depth and 90 m depth were used to feed the sub-header tanks. The time presented is the
 557 duration of the experimental deployment.

558



560

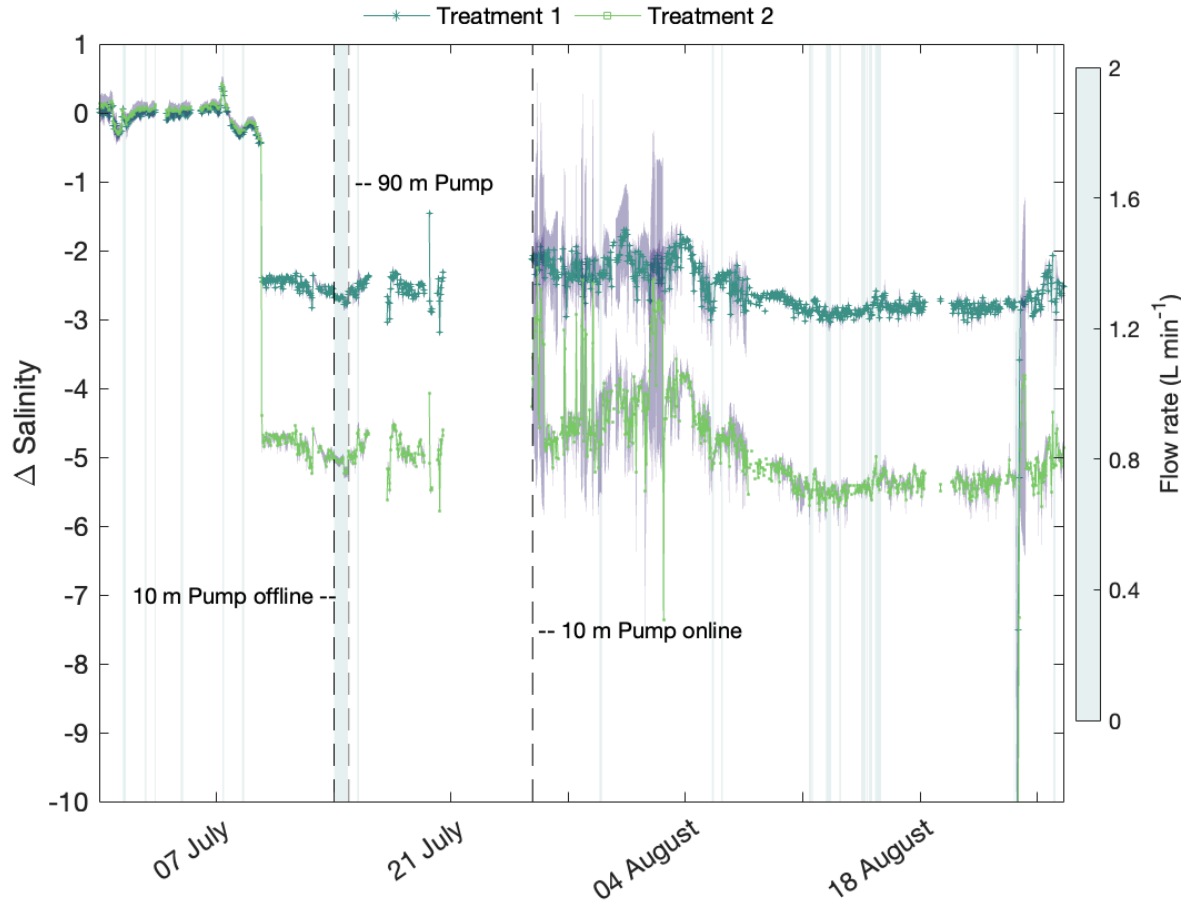
561 **Figure 3.** Mean (across triplicated mesocosms) temperature (°C; **a**) and salinity (**b**) values
 562 measured every minute over a 60 d period (including 6 day period before the start of the
 563 experiment) for the control (blue), and for treatments 1 – 3 (dark green, light green, and yellow,
 564 respectively).

565

566

567

568



569

570 **Figure 4.** The hourly mean (across triplicated mesocosms) salinity offsets for the experimental
 571 period. Dark green is treatment 1 and light green is treatment 2. The purple shaded region around
 572 the mean is the standard deviation and the heatmap isoclines (blue shaded regions) are the
 573 instances when flow rates $\leq 2 \text{ L min}^{-1}$. Dashed black lines indicate periods when the pump at 10
 574 m depth and 90 m depth were used to feed the sub-header tanks.

575

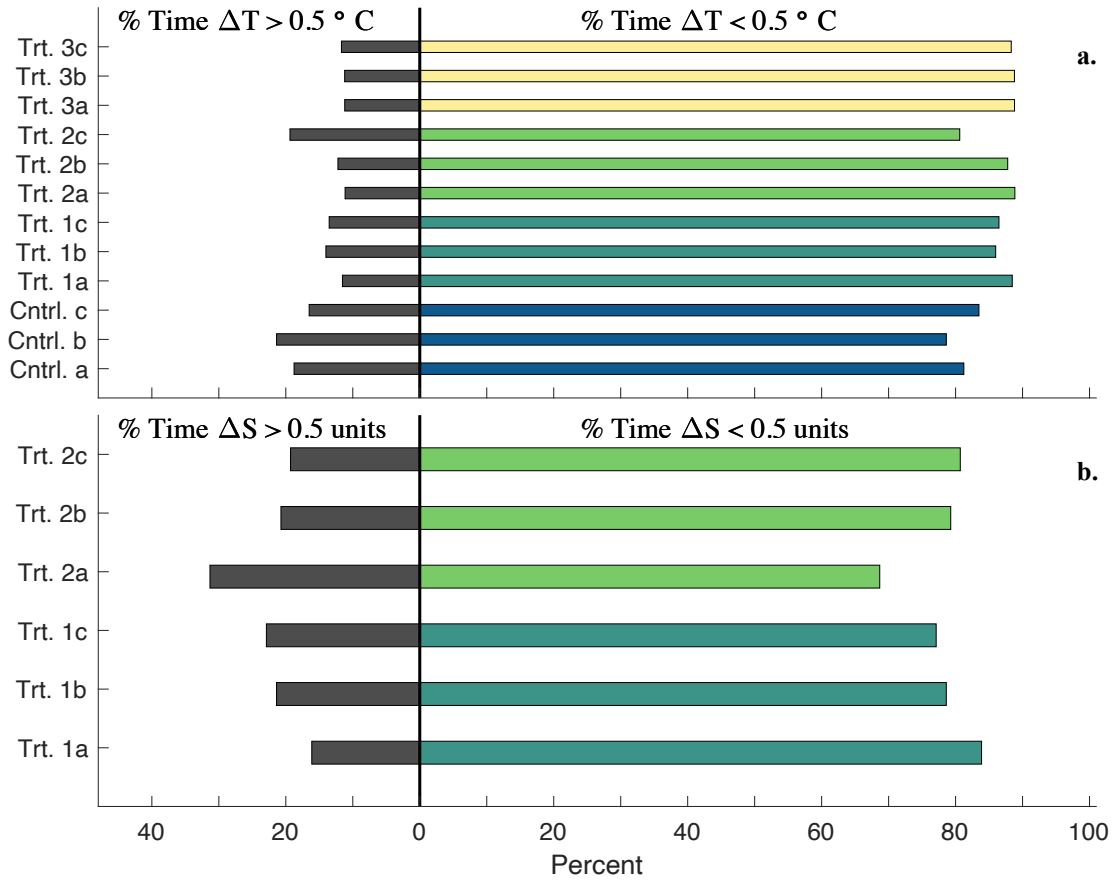
576

577

578

579

580



581

582

Figure 5. Percent time each mesocosm experienced a deviation > (black bars) or < (colored

583

bars) 0.5°C (ΔT; **a**) or 0.5 in salinity (ΔS; **b**) when flow rates were above 2 L min⁻¹. Cntrl. and

584

Trt. abbreviations are the control and treatments, respectively. This excludes the period when

585

using the 90 m pump (12 d), but accounts for 42 days out of the 54-day experiment. Bar color

586

indicates different treatment groups, as shown on the y-axes.

587

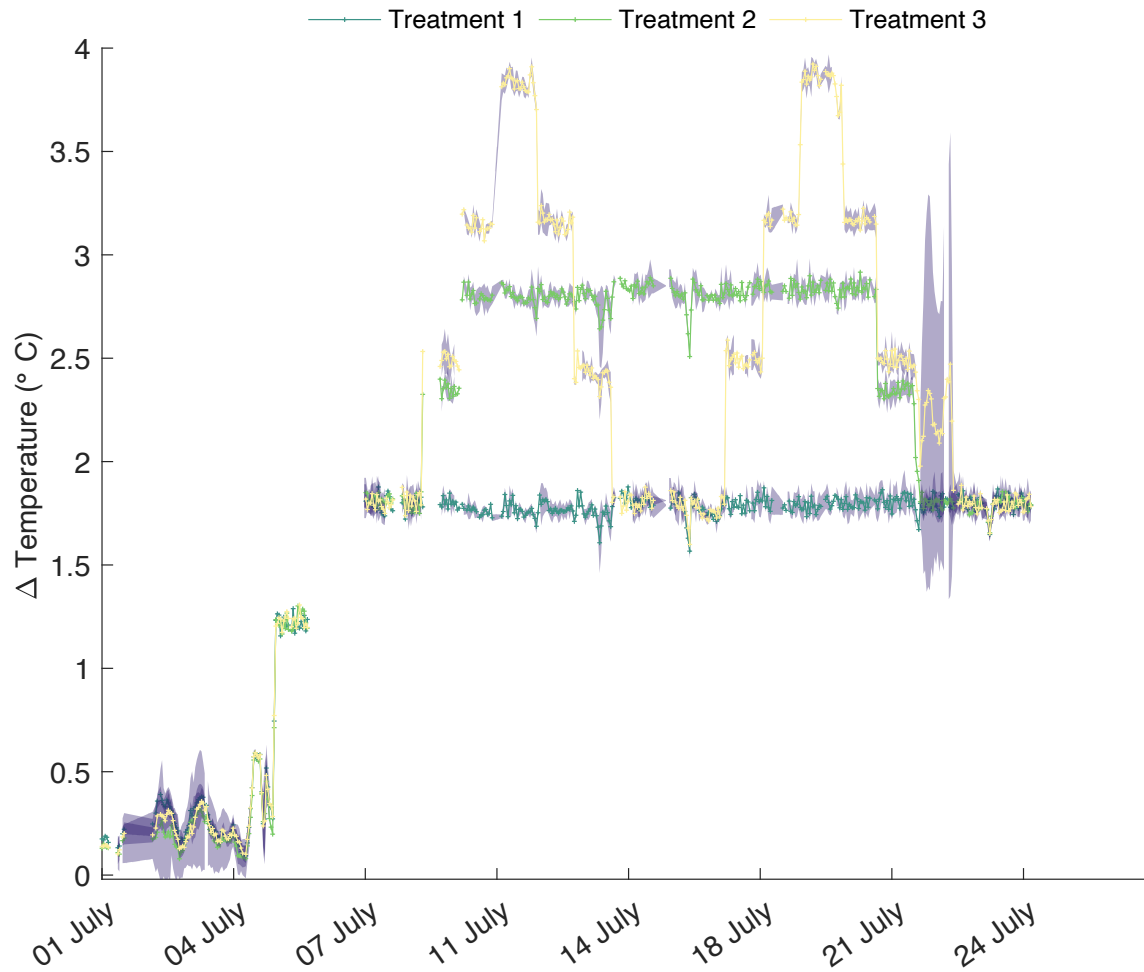
588

589

590

591

592



593

594 **Figure 6.** The hourly mean temperature offsets (Δ Temperature) during the 2nd deployment of
 595 SalTExPreS in the summer of 2022 in Tromsø (Norway) performing a variation of heatwave
 596 scenarios with three experimental treatments 1 – 3. Treatment 1 is a constant high temperature (+
 597 1.76°C), treatment 2 is a low frequency (1 heatwave) and medium magnitude offset (+ 2.81°C),
 598 while treatment 3 is a high frequency (2 heatwaves) and magnitude offset (+ 3.86°C). The purple
 599 shaded region around the mean is the standard deviation.

600

601

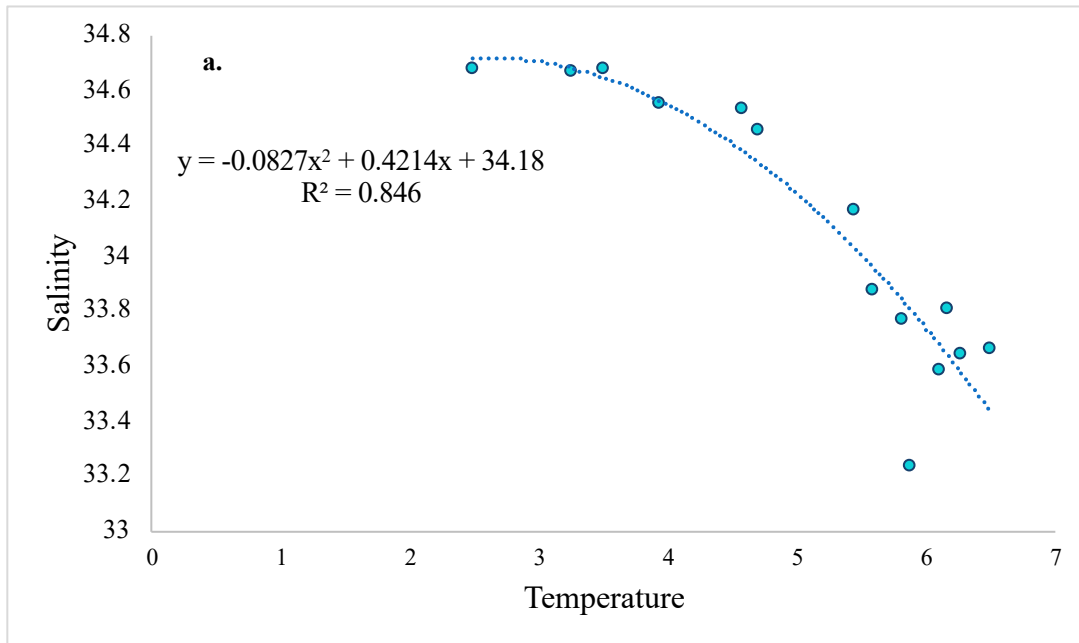
602

603

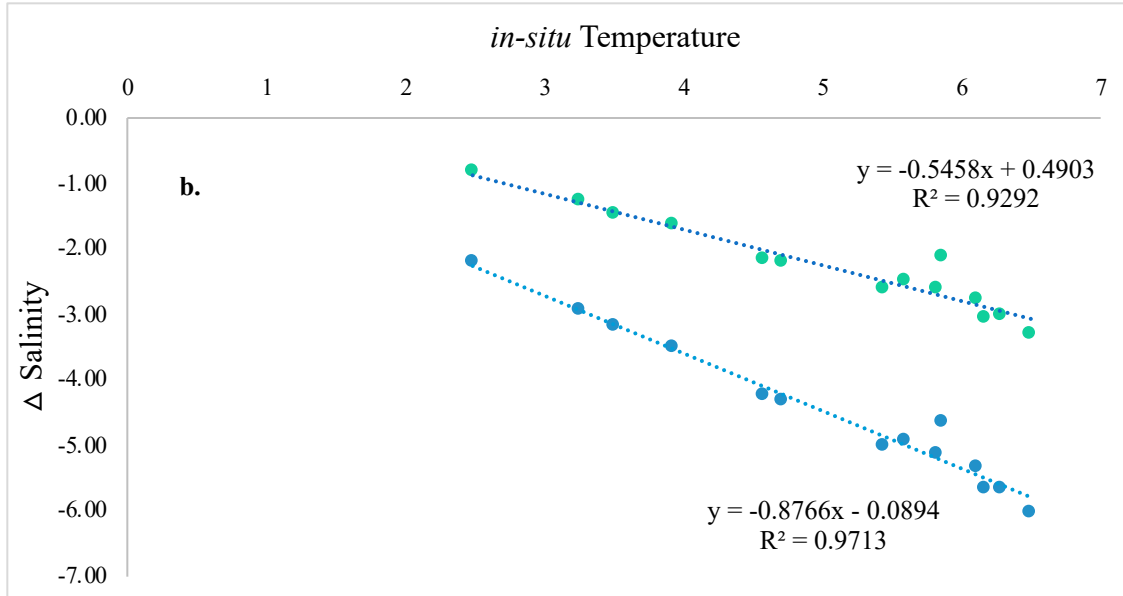
604 **Appendix**

605 **A1. Calculation of Salinity Offset**

606 In the summer of 2020—weeks 22 to 35— the mean temperature at 11 m displayed a range from
607 2.48 – 6.28, with salinity values ranging from 34.67 measured at the minimum 2.48°C and 33.63
608 measured at 6.28°C (Fig. A1a). The correlation was best fit with a 2nd order polynomial. To
609 project the salinity offset at a future temperature based on this 2nd order polynomial fit,
610 temperatures of + 3.3 and 5.3°C (SSP2-4.5 and SSP5-8.5, respectively) were added to *in-situ*
611 fjord temperatures and salinity was calculated based on the 2nd order polynomial. These
612 estimated salinity values were then subtracted from the mean salinity values observed (y-axis,
613 Fig. A1a) in summer 2020 in order to calculate a delta salinity value for the SSP2-4.5 and SSP5-
614 8.5 scenarios. The relationship between these estimated delta salinity values and the mean *in-situ*
615 temperature (y-axis, Fig. A1a) displayed a robust linear relationship (Fig A1b).



616



617

618 **Figure A1.** Relationship between temperature and salinity in summer 2020 weeks 22 – 35 in Ny-
 619 Ålesund, Svalbard (a). Relationship between estimated delta salinity and *in-situ* temperature,
 620 where delta salinity was calculated as the difference between the current mean salinity and the
 621 salinity estimated at the temperature increase projected for SSP2-4.5 (green dots) and SSP5-8.5
 622 (blue dots) scenarios (b).

623

624

625

626

627

628

629

630

631

632

633 **Table A1. Parts list with manufacturer model numbers.**

| Group | Item | Supplier/manufacturer | Model / details | Quantity |
|---------------------------|-------------------------------|--|---------------------------------|----------|
| Hydraulic system | | | | |
| | Mesocosms | home made | 1000 L fiber glass | 12 |
| | Seawater pump | NPS, BradFord, UK | Albatros F13T | 1 |
| | PVC-U tubing and fittings | | 20mm, 32mm & 50mm diameter | — |
| | Insulated flexible hose | | 19mm diameter | 100 m |
| Sensors | | | | |
| | Conductivity / temperature | Aqualabo, Champigny sur Marne, France | PC4E | 12 |
| | Oxygen | Aqualabo, Champigny sur Marne, France | PODOC | 12 |
| | Pressure | Siemens, Munich, Germany | 7MF1567-3BE00-1AA1 | 3 |
| | Flow rate | IFM, Essen, Germany | SV3150 | 12 |
| Actuators | | | | |
| | Pressure regulation valves | BELIMO, Hinwil, Switzerland | R2025-10-S2 with LR24A-SR motor | 3 |
| | Temperature regulation valves | BELIMO, Hinwil, Switzerland | R3015-10-S2 with LR24A-SR motor | 12 |
| | Salinity regulation valves | BELIMO, Hinwil, Switzerland | R2015-10-S2 with LR24A-SR motor | 6 |
| Automation cabinet | | | | |
| | Cabinet | Fibox, Espoo, Finland | FIB8120017N | 1 |
| | Security switch | KRAUS-NAIMER, Karlsruhe, germany | KNA002245 | 1 |
| | 12 vdc power supply | TDK Lambda, New York, USA | LAMDRL30-12-1 | 1 |
| | 24vdc power supply | TDK Lambda, New York, USA | LAMDRB240-24-1 | 1 |
| | PLC | Industrial Shields, Barcelona, Spain | Mduino-42+ | 4 |
| | Ethernet switch | HIRSCHMANN-INET, Neckartenzlingen, Germany | HIR942132002 | 1 |

634

635 **A2. Temperature and Salinity Regulation**

636 Accurate temperature and salinity regulation was managed using the software PID (proportional
637 integral derivative) controller on the corresponding Programmable Logic Controller (PLC). The
638 PLC operated in PoE mode (power over ethernet) which builds a local area network (LAN)
639 enabling use of Ethernet data cables to carry electrical power. The PID controller measures the
640 difference between the measured value and the nominal value (i.e., the error). This calculates the
641 position and adjustment of the valve opening by multiplying the error, the integral of this error,
642 and the derivative of the error over time, by previously determined coefficients K_p (proportional
643 gain), K_i (integral gain) and K_d (derivative gain), respectively. These coefficients were obtained
644 experimentally using the empirical method of Ziegler & Nichols (1943). These coefficient values
645 may differ from one condition to another.

646

647 **A2.1. Pressure and Flow Regulation**

648

649 Each sub-header tank inlet line of ambient, chilled and warmed seawater had its own pressure
650 regulation system enabling equivalent pressure levels to be maintained. This regulation process
651 aided in the ability to adjust flow rates for all mesocosms by using the hand-crank valves (Fig.
652 1). The system consisted of an analog pressure sensor (Siemens© 7MF1567-3BE00-1AA1) and
653 a two-way analog valve (BELIMO© R2025-10-S2 with LR24A-SR motor). The pressure
654 sensors were placed in-line directly after water from each sub-header tank passed through a
655 regulator valve. The sensor ensured that pressure for each line was maintained at 0.3 bars by
656 transmitting data to the system which then regulated the valve opening position of the incoming
657 flow. A nominal pressure for all three sensors was predetermined during flow rate test trials. This

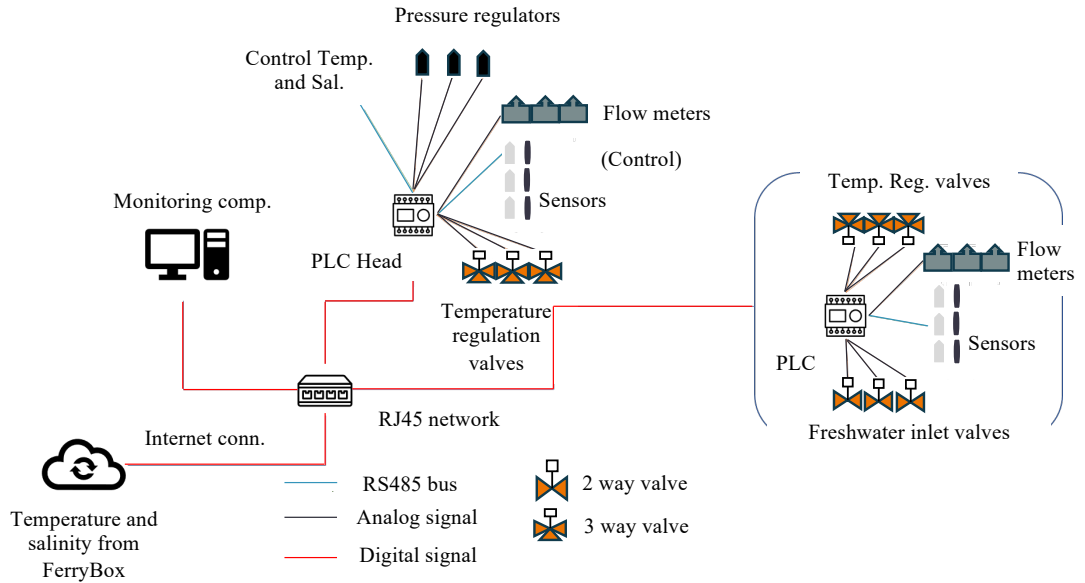
658 process took place during the setup of the system where the valve opening was adjusted using a
659 PID regulator (see A2) to maintain the defined nominal pressure.

660
661 **A2.2 Automation**

662 The automation was performed using 4 Industrial Arduino-based PLCs (Industrial shields©
663 Mduino-42+), with an individual PLC regulating the control and each treatment 1 – 3,
664 respectively. Each PLC was responsible for logging data and regulating a specific experimental
665 condition. The PLC regulating the control—identified as the Head PLC—was the primary device
666 responsible for communication with the branched PLCs and the monitoring computer (Fig. A2).
667 All monitoring was performed on a PC Windows application (Section A3) and responsible for:
668 (1) reading data received from the PLCs, (2) reading *in-situ* data received from the internet, (3)
669 displaying live data, (4) logging data and sending it to an FTP server, and (5) sending settings
670 and commands to the PLCs. Communication between the PLCs and the PC was ensured using
671 http WebSocket protocol on RJ45 ethernet cables. The communication between the PLCs and the
672 conductivity-temperature and oxygen sensors, flow rate sensors, and regulation valves was
673 executed using a half duplex RS485 (2 wires) protocol, with an analog 4-20mA and an analog 0-
674 10V signal, respectively. All PLCs and wired communication lines were housed in an electrical
675 box installed to an IP68 Fibox enclosure with a 400 V (3P+N+E) 32 A security switch (Fig. A6).
676 All the automation elements use low tension (12 Vdc or 24 Vdc) through circuit breakers and
677 fuses. The electrical box was protected with a 220 V socket.

678

Automation Hardware Architecture



679

680 **Figure A2.** Diagram and flow-chart of the automation system.

681

682

683

684

685

686

687

688

689

690

691

692 **A3. Software Development**

693 The code for the application was written in C/C++. The code uses publicly available Arduino
694 libraries (<https://www.arduino.cc/reference/en/libraries/>) as well as originally designed libraries.
695 All code is available on Github (<https://github.com/purrutti/FACEIT>). The code is divided into
696 two pathways: ‘Master.ino’ for the Head PLC, and ‘Regul_condition.ino’ for the Branched
697 PLCs. A description of the main functions applied in the code for programming the system
698 regulation and features are listed in Table A3.

699

700

701

702

703

704

705

706

707

708

709

710

711

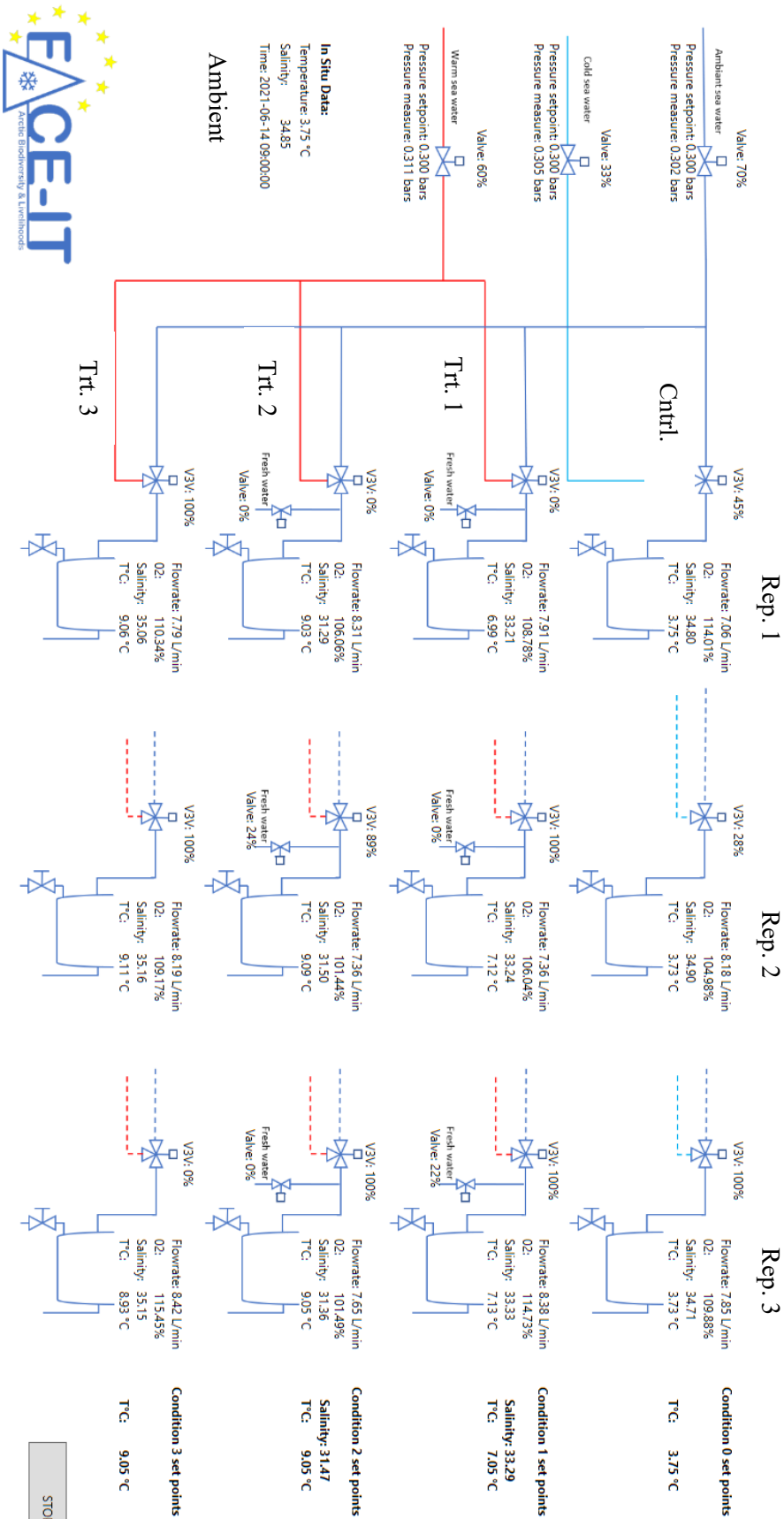
712

713

714

715 **Table A3.** Functions used for programming of software.

| Function | Operation | Arcellery field Sender ID | Arcellery field Command # |
|--|---|---|--|
| <i>RTC/read()</i> | The PLCs are equipped with a RTC chip and battery to keep track of the date. Once set on commissioning, <i>RTC.read()</i> returns the current date and time. This function loops through each sensor connected on the RS485 bus. Each Mesocosm has two sensors (O2 and Conductivity/Salinity), so each PLC has 6 sensors connected on its bus. | | |
| <i>readMesosensors()</i> | - O2 sensors have addresses ranging from 10 to 12, for mesocosms 0 to 2 of the scenario, respectively. - PC4E sensors have addresses ranging from 30 to 32, for mesocosms 0 to 2 of the scenario, respectively. - Sensors are requested individually and in sequence. A request is made every 200 ms. | | |
| <i>websocket/loop()</i> | This is a callback function responsible for dealing with the WebSocket communication. The master PLC is the WebSocket server. It listens to slave PLCs requests and to the monitoring PC requests. Requests are JSON formatted. They always contain <i>entityId</i> / <i>fields</i> : <i>senderID</i> (ID of the entity sending the request), <i>condID</i> (ID of the requested entity), <i>command</i> (command type of the request). They optionally can also contain a « time » field: Unix-like timestamp (number of seconds since 01-01-1970) | Head PLC (ID = 0) Branched PLCs (ID = 1-3) Monitoring PC (ID = 4) | Request params: <i>sepoints</i> , <i>PID settings</i> (# = 0) Request data: <i>measurement values</i> , <i>regulation outputs</i> (# = 1) Send Params: response to a « request params » request (# = 2) Send Data: response to a « request data » request (# = 3) Calibrate sensor: request for calibrating sensor to specified value (# = 4) Request Head data: specific data measured by Head PLC (pressure & flowrates) (# = 5) Send Head data: a response to a « request Head data » request (# = 6) |
| <i>regulationTemperature()</i> | This function is responsible for the temperature regulation of the mesocosm. It sets the corresponding three-way valve position using a 0-10V analog signal. The function first checks if the regulation is in « manual override » mode. If so, it applies the override setpoint. If not, it reads the temperature measure in the mesocosm, compares it with the setpoint, and uses the PID settings to set the valve position. | | |
| <i>checkMesocosms()</i> | This function loops through every mesocosm every 200 ms and reads analog signals (i.e., flowrates and pressure readings). | | |
| <i>regulationPressure()</i> <i>Only for HEAD PLC</i> | This function is responsible for the pressure regulation of the mesocosm. It sets the corresponding three-way valve position using a 0-10V analog signal. The function first checks if the regulation is in « manual override » mode. If so, it applies the override setpoint. If not, it reads the pressure measure in the mesocosm, compares it with the setpoint, and uses the PID settings to set the valve position. | | |
| <i>printOASD()</i> <i>Only for HEAD PLC</i> | Master PLC is equipped with a microSD card, on which data from all mesocosms is logged every 5 seconds, in one csv file per day. This is for security only, as the microSD card is not easy to remove from the PLC casing. It should not be removed before the end of the experiment. | | |
| <i>regulationSalinite()</i> <i>Only for Branched PLCs</i> | This function is responsible for the salinity regulation of the mesocosm. It sets the corresponding three-way valve position using a 0-10V analog signal. The function first checks if the regulation is in « manual override » mode. If so, it applies the override setpoint. If not, it reads the salinity measure in the mesocosm, compares it with the setpoint, and uses the PID settings to set the valve position. | | |



718 **Figure A3.** Application interface displaying real-time monitoring of ambient conditions as well
719 and control (Cntrl.), and treatment (Trt.) conditions for each replicate (Rep.) in each mesocosm.

720

721

722

723

724

725

726

727

728

729

730

731

732

733

734

735

736

737

738

739

740

741 **A4. Menu bar of PC application**

742 From the interface, the user sets the temperature condition and associated salinity offset, IP
743 address and logging parameters, sensor calibration settings, and nominal pressure (Fig. A4).

744 Within the menu bar several tabs permit the setup of the project: file, settings, maintenance, and
745 data. Under ‘file’ the system can be manually connected to, or disconnected from, the PLCs.

746 Connection is usually maintained automatically. The ‘settings’ tab displays the application and
747 experimental setting options (Fig. A4.1 a – c). All the settings of the project are stored on the
748 computer (found in ‘application settings’) that is running the application, which include:

- 749 i. *Master IP address*: The IP Address of the Master PLC (centralizing all the data).
- 750 ii. *Data Query Interval*: Frequency of queries from the application to the master PLC.
- 751 iii. *Data Log Interval*: Number of minutes between logs to file.
- 752 iv. *Data Base File Path*: Directory and base filename of the csv data files.
- 753 v. *FTP Username, Password, Path*: FTP settings for sending the data file every hour.
- 754 vi. *InfluxDB Settings*: For Live Monitoring and local storage of the data.

755 Under ‘experimental settings’, the programmed specificities and regulation of the treatment
756 conditions can be adjusted. This includes programming the nominal pressure (all main inflow
757 lines), temperature and the salinity-temperature relational equation (on a different tab selected
758 from dropdown), as well as adjusting the K_p , K_i & K_d coefficients for the regulation (see section
759 2.3.1). The nominal temperature is provided by the data received from the ferry-box, however
760 this can be overridden if needed. The « Save to PLC » button sends the values to the
761 corresponding PLC and saves the data, while the « Load from PLC » button loads the settings
762 from the PLC. For the purposes of this experiment, the nominal salinity was calculated based on
763 a delta salinity for treatments 1 and 2 which were derived from the linear relationship with

764 temperature (see section 2.3.1). This can also be overridden if needed by selecting the manual
765 override box.

766 The ‘maintenance’ tab is where sensor calibration and communication ‘Debug’
767 operations can be executed (Fig. A4 d, e). Calibration can be performed for each sensor deployed
768 in each mesocosm, and uses a 2-point calibration for temperature and % oxygen. The salinity
769 calibration is done by setting the conductivity value corresponding to a temperature of 25°C
770 rather than the *in situ* measured temperature. The conductivity value is programmed as $\mu\text{S cm}^{-1}$.
771 The communication process for sensor calibration is between 5 to 10 seconds. The final option in
772 the menu is the ‘data’ tab which displays the historical and live data. The historical data can be
773 interfaced to an html site if desired.

774

776 **Figure A4.** Operation windows for the application and experimental settings (**a-c**). These
777 windows are found under the ‘settings’ tab. Operation windows for sensor calibration and
778 debugging (**d, e**). These are found under the ‘maintenance’ tab.

779

780

781

782

783

784

785

786

787

788

789

790

791

792

793

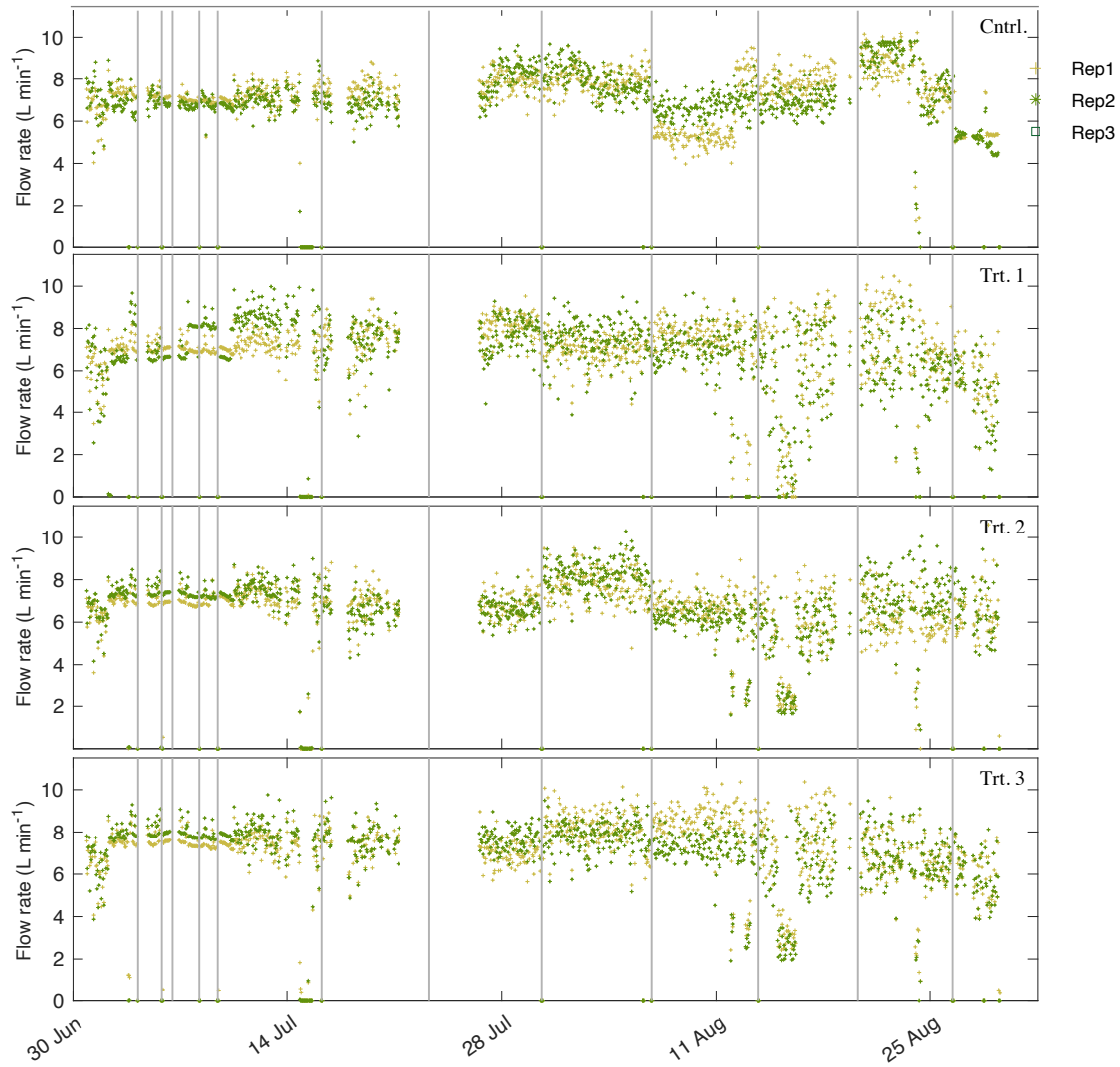
794

795

796

797

798



800

801 **Figure A5.** Flow rates for control and treatments 1-3 for the entirety of the system deployment.

802 Black vertical lines are when incubations were performed and the system shut-off for a period of

803 3 h. Flow rates went to zero at these times.

804

805

806

807



808

809 **Figure A6.** All 12 mesocosms are displayed (upper left photo) with the inside of one mesocosm

810 (right photo) showing the oxygen (silver) and temperature/conductivity sensors along with the

811 photosynthetically active radiation (PAR) logger (bottom right photo).

812

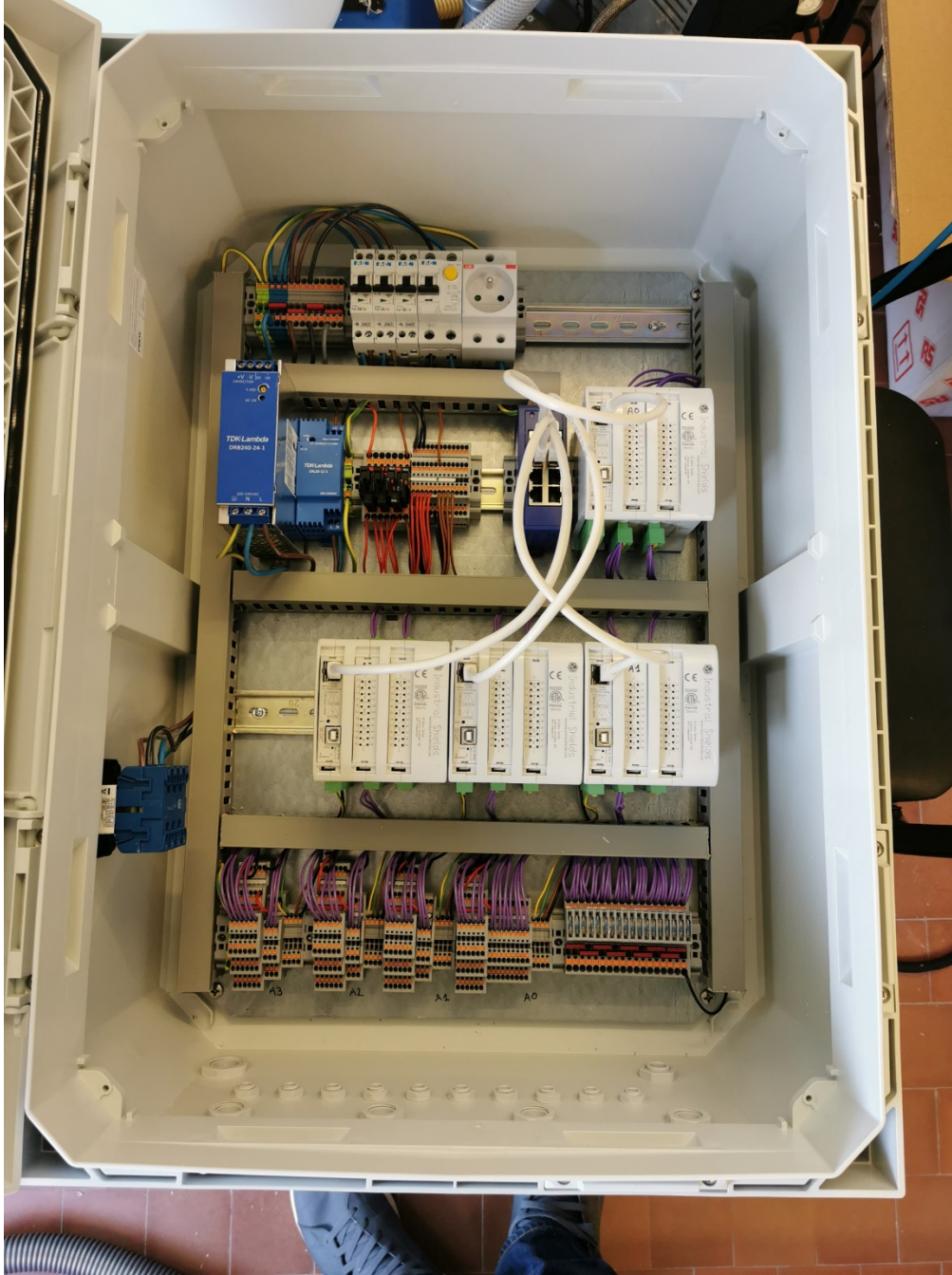
813

814

815

816

817



818

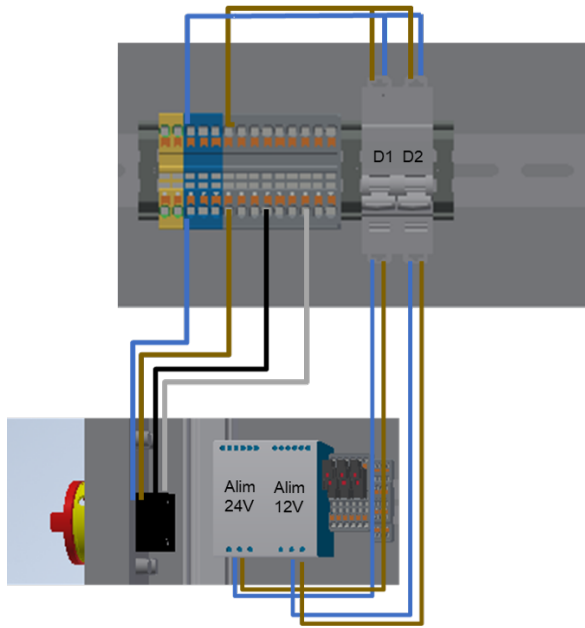
819 **Figure A7.** Electrical cabinet used for SalTExPreS

820

821

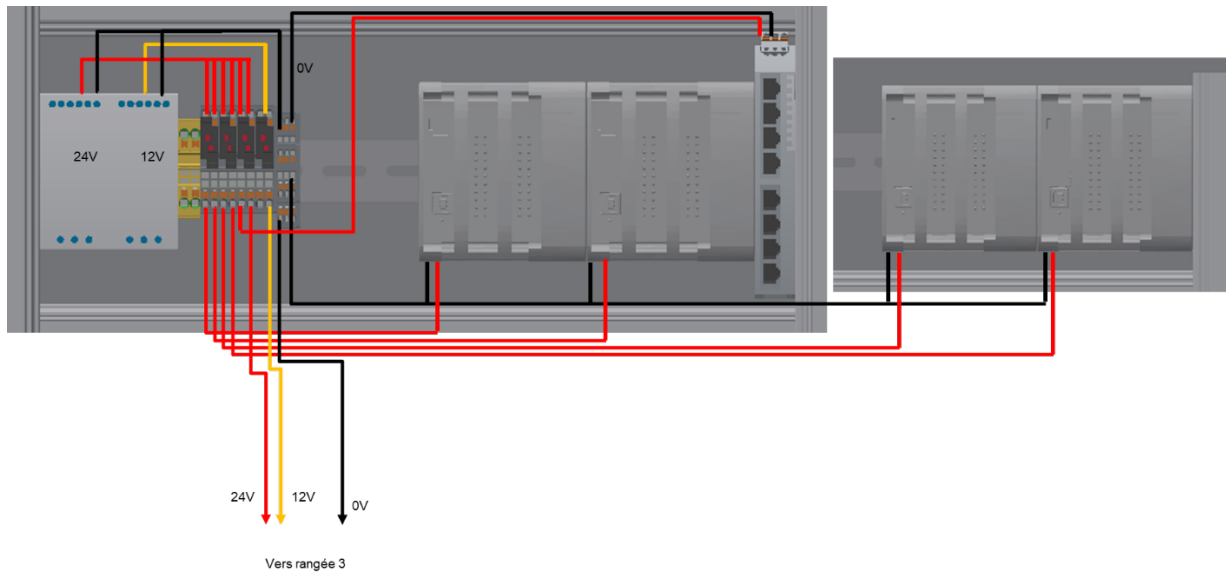
822

823



D1: Alim 24Vdc
 D2: Alim 12Vdc

824



825

826 **Figure A8.** Electrical schematic for wiring within the electrical box.

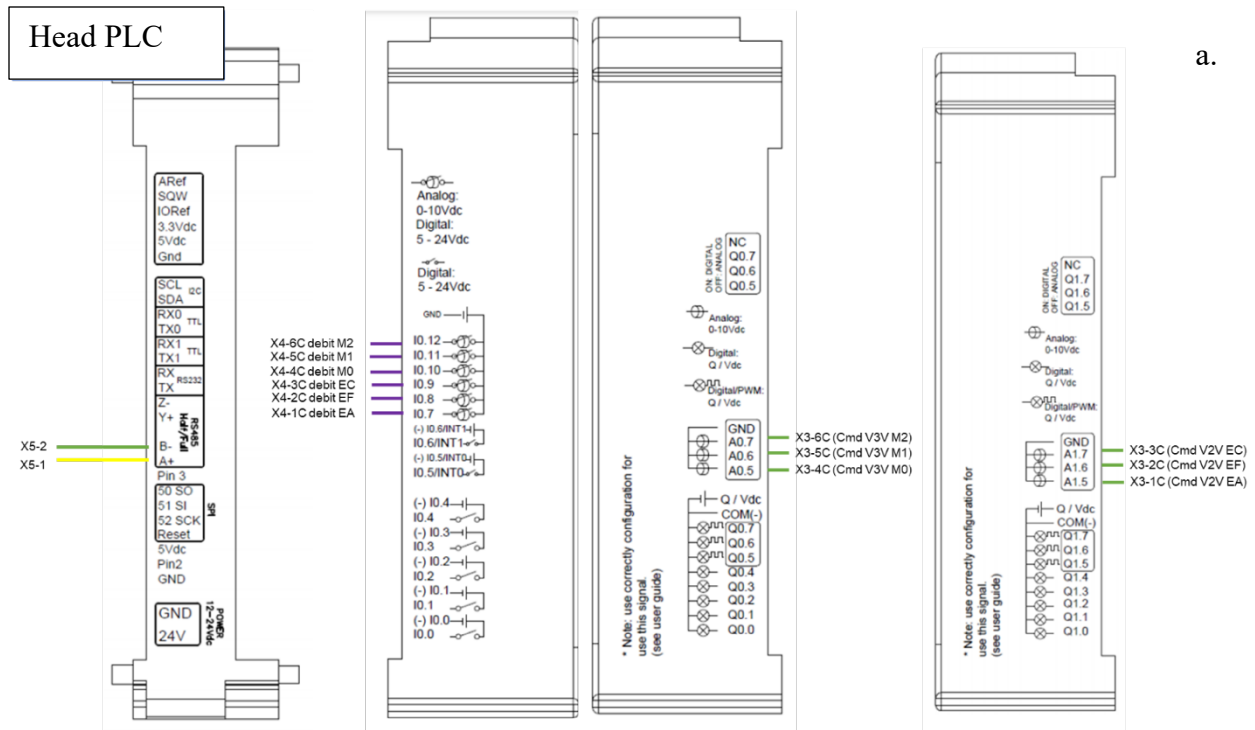
827

828

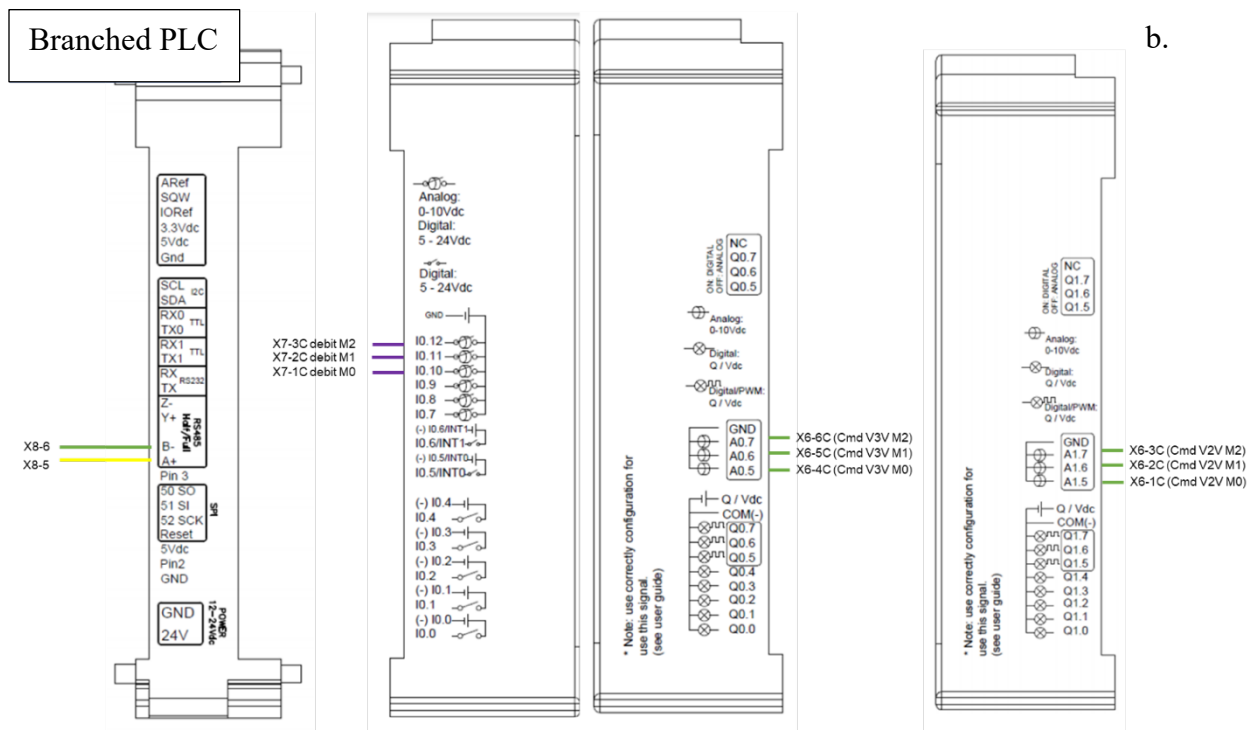
829

830

831



832



833

834 **Figure A9.** PLC controller diagram for Head (a) and Branched (b) operations.

835

836